

## SIGNALLING

# $\beta$ 2-adrenergic stimulation potentiates spontaneous calcium release by increasing signal mass and co-activation of ryanodine receptor clusters

Carme Nolla-Colomer<sup>1</sup> | Sergi Casabella-Ramon<sup>2,3</sup> | Veronica Jimenez-Sabado<sup>3,4</sup> | Alexander Vallmitjana<sup>1</sup> | Carmen Tarifa<sup>2,3</sup> | Adela Herraiz-Martínez<sup>2,3</sup> | Anna Llach<sup>3</sup> | Manel Tauron<sup>5</sup> | Jose Montiel<sup>5</sup> | Juan Cinca<sup>3,6</sup> | S. R. Wayne Chen<sup>7</sup> | Raul Benitez<sup>1</sup> | Leif Hove-Madsen<sup>2,3</sup> 

<sup>1</sup>Department Automatic Control, Univ. Politècnica de Catalunya, Barcelona, Spain

<sup>2</sup>Biomedical Research Institute Barcelona, IIBB-CSIC, Barcelona, Spain

<sup>3</sup>IIB Sant Pau, Barcelona, Spain

<sup>4</sup>CIBERCV, Madrid, Spain

<sup>5</sup>Department of Cardiac Surgery, Hospital de la Santa Creu i Sant Pau, Barcelona, Spain

<sup>6</sup>Universitat Autònoma de Barcelona, Barcelona, Spain

<sup>7</sup>Department of Physiology and Pharmacology, University of Calgary, Alberta, Canada

## Correspondence

Leif Hove-Madsen, Cardiac Rhythm and Contraction, Biomedical Research Institute Barcelona (IIBB-CSIC), Hospital de la Santa Creu i Sant Pau, St Antoni M<sup>a</sup> Claret 167, 08025 Barcelona, Spain.  
Email: leif.hove@iibb.csic.es

## Funding information

This work was supported by grants from the Spanish Ministry of Science and Innovation PID2020-116927RB-C21 and SAF2017-88019-C3-1R (to LHM) and SAF2017-88019-C3-3R (to RB); from Fundació Marató TV3, Marató-2015-2030 (to LHM); from Generalitat de Catalunya SGR2017-1769 (to LHM); from the Natural Sciences and Engineering Research Council of Canada (to SRWC); from the Canadian Institutes of Health Research (to SRWC); from the Heart and Stroke Foundation Chair in Cardiovascular Research (to SRWC), and from Spanish Ministry of Health

## Abstract

**Aims:** It is unknown how  $\beta$ -adrenergic stimulation affects calcium dynamics in individual RyR2 clusters and leads to the induction of spontaneous calcium waves. To address this, we analysed spontaneous calcium release events in green fluorescent protein (GFP)-tagged RyR2 clusters.

**Methods:** Cardiomyocytes from mice with GFP-tagged RyR2 or human right atrial tissue were subjected to immunofluorescent labelling or confocal calcium imaging.

**Results:** Spontaneous calcium release from single RyR2 clusters induced  $91.4\% \pm 2.0\%$  of all calcium sparks while  $8.0\% \pm 1.6\%$  were caused by release from two neighbouring clusters. Sparks with two RyR2 clusters had 40% bigger amplitude, were 26% wider, and lasted 35% longer at half maximum. Consequently, the spark mass was larger in two- than one-cluster sparks with a median and interquartile range for the cumulative distribution of  $15.7 \pm 20.1$  vs  $7.6 \pm 5.7$  a.u. ( $P < .01$ ).  $\beta$ 2-adrenergic stimulation increased RyR2 phosphorylation at s2809 and s2815, tripled the fraction of two- and three-cluster sparks, and significantly increased the spark mass. Interestingly, the amplitude and mass of the calcium

See related editorial: Roderick HL. 2022. The cardiomyocyte firestarter—RyR clusters ignite their neighbours after augmentation of Ca<sup>2+</sup> release by  $\beta$ -stimulation *Acta Physiol* (Oxf). e13798.

Raul Benitez, Leif Hove-Madsen co-senior authors.

This is an open access article under the terms of the Creative Commons Attribution-NonCommercial-NoDerivs License, which permits use and distribution in any medium, provided the original work is properly cited, the use is non-commercial and no modifications or adaptations are made.

© 2021 The Authors. *Acta Physiologica* published by John Wiley & Sons Ltd on behalf of Scandinavian Physiological Society.

and Consume CB16/11/00276 (to JC). SC was the recipient of a predoctoral grant (FPU18/01250) from the Spanish Ministry of Science and Innovation, and AL received a PERIS SALUT-16 grant from Generalitat de Catalunya.

released from a RyR2 cluster were proportional to the SR calcium load, but the firing rate was not. The spark mass was also higher in 33 patients with atrial fibrillation than in 36 without ( $22.9 \pm 23.4$  a.u. vs  $10.7 \pm 10.9$ ;  $P = .015$ ).

**Conclusions:** Most sparks are caused by activation of a single RyR2 cluster at baseline while  $\beta$ -adrenergic stimulation doubles the mass and the number of clusters per spark. This mimics the shift in the cumulative spark mass distribution observed in myocytes from patients with atrial fibrillation.

#### KEYWORDS

calcium spark, cardiac myocyte, confocal imaging, ryanodine receptor, sarcoplasmic reticulum,  $\beta$ -adrenergic

## 1 | INTRODUCTION

Ventricular tachycardia and atrial fibrillation (AF) have been associated with an elevation of the incidence of calcium sparks and calcium waves,<sup>1</sup> which in turn have been shown to induce afterdepolarizations<sup>2</sup> capable of initiating triggered activity and arrhythmia.<sup>3</sup> Among the mechanisms thought to underlie a higher incidence of spontaneous calcium release, RyR2 phosphorylation at both s2808<sup>4,5</sup> and s2814<sup>6,7</sup> that increases the RyR2 open probability<sup>4</sup> has been proposed to facilitate the fusion of calcium sparks into calcium waves.<sup>2</sup> However, it has also been shown that overexpression of phospholamban in transgenic mice with the R4496C mutation splits large calcium waves in the R4496C mutants into a large number of miniwaves and calcium sparks, which prevents arrhythmogenesis in the double mutant mice.<sup>8</sup> Thus, the incidence of calcium sparks or the magnitude of passive calcium leak alone cannot be used unequivocally to estimate the risk of arrhythmia. Instead, the ability of individual RyR2 clusters to propagate the calcium signal to neighbouring clusters or to break the propagation of larger calcium release events might be determinant.

Because sparks are expected to occur when some or all of the RyR2s in a RyR2 cluster opens, the properties of a spark, and its ability to induce calcium release from neighbouring RyR2 clusters, is expected to depend on the number of RyR2s in a cluster and the fraction of RyR2 that opens.<sup>9,10</sup> Presumably, the ability of a spark to propagate its calcium signal will also depend on the number of RyR2 clusters that contribute to the spark transient. In this regard, local non-propagating calcium release events have been classified according to the magnitude of the resulting calcium transient as calcium quarks,<sup>11</sup> calcium sparks<sup>12</sup> or macrosparks.<sup>13,14</sup> Moreover, in a sheep model of AF this arrhythmia was associated with RyR2 cluster fragmentation and redistribution.<sup>14</sup> However, little is known about the relationship between the activation of individual RyR2

clusters and the formation of sparks or their fusion into calcium waves capable of triggering spontaneous membrane depolarizations.

We hypothesized that the ability of a local calcium release event to trigger neighbouring RyR2 clusters would depend on its calcium signal mass, which integrates the amplitude, width and duration of the calcium signal. To test this hypothesis, we used transgenic mice with GFP-tagged RyR2s that allowed us to measure calcium release in individual RyR2 clusters and determine how the signal mass or other features of the calcium release event affects the activation of neighbouring RyR2 clusters at baseline and upon beta-adrenergic stimulation, which is known to induce cardiac arrhythmia and arrhythmic responses in isolated cardiomyocytes. Moreover, because atrial fibrillation (AF) has been associated with changes in the frequency and properties of calcium sparks and attributed to increased RyR2 phosphorylation, we also wanted to explore whether AF was associated with changes in the calcium spark mass comparable to those observed under beta-adrenergic stimulation.

## 2 | RESULTS

### 2.1 | Properties, mass and clustering of calcium signals from individual RyR2 clusters

We analysed a total of 3335 RyR2 clusters in 64 cells from 16 mice. Overall, 228 of the 3335 clusters were activated at least once, giving rise to 467 sparks caused by the activation of a single RyR2 cluster (Figure 1A top) corresponding to  $91.4\% \pm 2.0\%$  of all sparks. Moreover, 53 sparks were caused by the simultaneous activation of two RyR2 clusters (Figure 1A bottom) corresponding to  $8.0\% \pm 1.6\%$  of all sparks. From the 53 double-cluster sparks, 45 (84.9%) were caused by RyR2 activations on the same Z-line while

only 8 (15.1%) sparks involved the activation of RyR2 clusters on different Z-lines. Figure 1B illustrates the relationship between single-cluster signals measured in a  $0.5 \times 0.5 \mu\text{m}^2$  region of interest (ROI) and the resulting spark signal measured in a  $4 \times 4 \mu\text{m}^2$  ROI. At baseline,

we found only 11 sparks resulting from the activation of three clusters. As expected, contour plots of the single- and double-cluster sparks had one and two local maxima (Figure 1C-D). Figure 1E shows the fraction of sparks with one and two RyR2 clusters. Figure 1F shows the

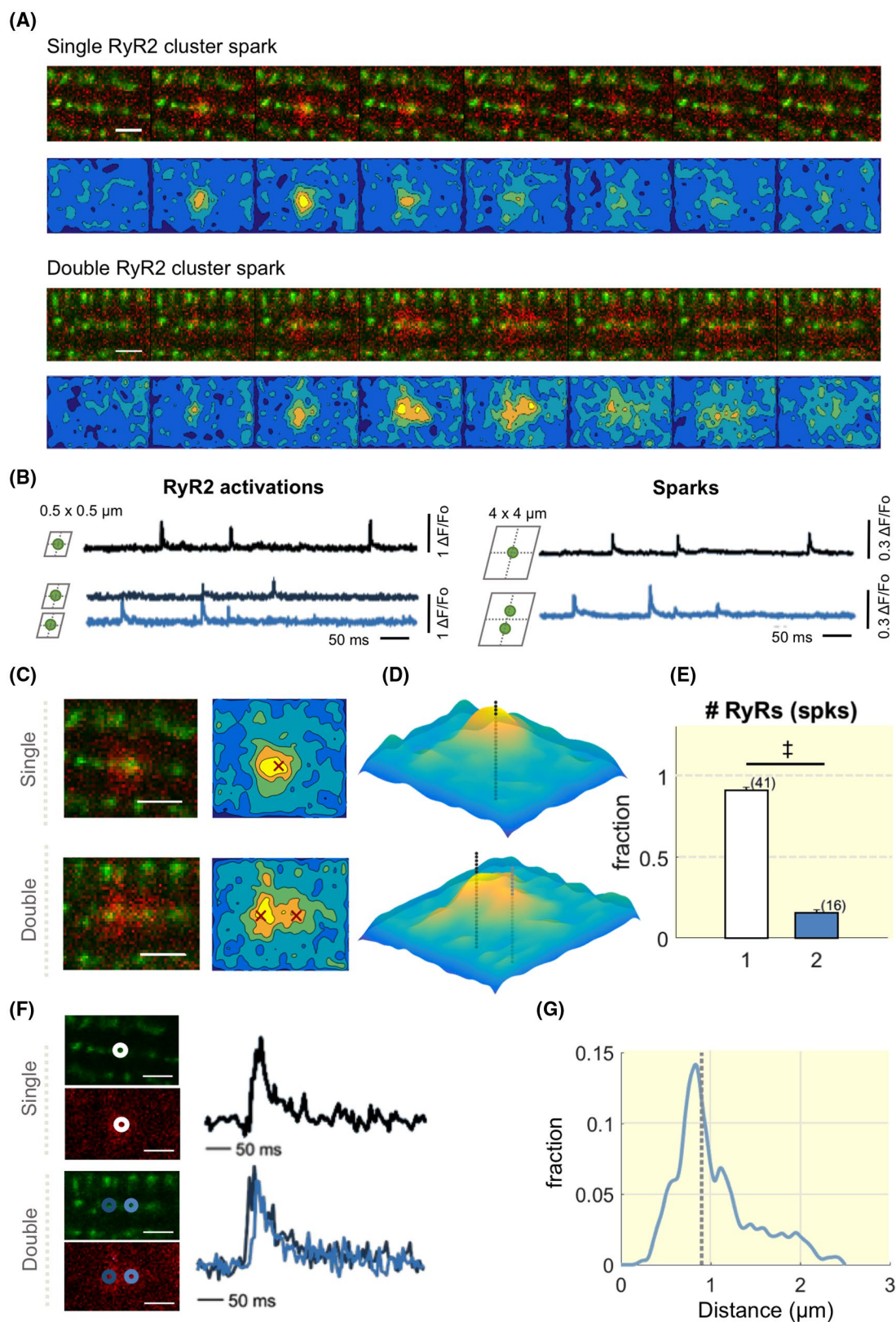


**FIGURE 1** Calcium sparks at baseline are caused by activation of a single or two RyR2 clusters. A, Superimposed image frames of GFP-tagged RyR2 clusters (green) and calcium spark signal (red). The colour-code map below images show the isolated calcium spark signal. Consecutive image frames are shown for a single (top panels) and a double RyR2 cluster spark (bottom panels). Image frames are separated by 8.32ms, white scale bars are 2  $\mu\text{m}$ . B, Calcium signal recordings from individual RyR2 clusters in  $0.5 \times 0.5 \mu\text{m}^2$  ROIs (left) and the resulting calcium spark signal in a  $4 \times 4 \mu\text{m}^2$  ROI (right) signals are shown for a single (black traces) and a double-cluster spark (blue traces). C-D, Two- and 3-D contour plots of single and double-cluster sparks. E, Fraction of sparks with 1 and 2 RyR2 clusters. F, Kinetics of calcium signals in individual RyR2 clusters from a single (top) and a double RyR2 cluster spark (bottom) Images show cluster location (green) and calcium signal (red). G, Distribution of distances to nearest RyR2 cluster. Dashed line indicates the median distance for all sparks. <sup>‡</sup>Indicate  $P < .001$  (rank-sum test). Number of cells from 16 mice is indicated in parenthesis

kinetics of calcium signals in clusters from a single and double-cluster spark. The mean time between the first and the second RyR2 cluster activation was  $12.47 \pm 1.78$  ms. The distance between clusters in a two-cluster spark was  $0.78 \pm 0.03 \mu\text{m}$  for those on the same Z-line and  $1.88 \pm 0.06 \mu\text{m}$  for those on different Z-lines (Figure 1G).

When comparing spatial and kinetic properties of single- and double-cluster sparks, we found that double-cluster sparks were wider (Figure 2A-D), lasted significantly longer (Figure 2E,F), and had larger spark amplitude than those from a single cluster (Figure 2G,H). We did not observe significant differences in the rate of rise (RoR),  $0.036 \pm 0.003$  ( $\Delta F/F_0$ )/ms vs  $0.040 \pm 0.006$  ( $\Delta F/F_0$ )/ms ( $P = .50$ ), or in the decay of the calcium sparks with time constants of  $67 \pm 10$  ms for single-cluster sparks and  $74 \pm 7$  ms for double-cluster sparks ( $P = .07$ ). Interestingly, a comparison of calcium signals in individual RyR2 clusters during the activation of a single or a two-cluster spark revealed no significant difference in the amplitude or duration of the calcium signals during the activation of a single- or a two-cluster event. Moreover, the event frequency was similar in RyR2 clusters that only gave rise to single-cluster sparks and in those clusters that also gave rise to two-cluster events (Figure S1).

Since the arrhythmogenic potential of spontaneous calcium release events depends on their ability to trigger neighbouring clusters, ie on the combination of their amplitude, width, and duration; we used the time integral of the calcium signal in a spark over the baseline containing ROI, namely the spark's mass, to achieve a measure of its arrhythmogenic potential (Figure 3A). Figure 3B shows that the mass of the calcium spark was  $9.1 \pm 1.0$  a.u. for single-cluster sparks and  $16.9 \pm 3.4$  a.u. for double-cluster sparks ( $P < .01$ ). Figure 3C shows the probability distribution of the calcium spark mass for all sparks from single- or double-cluster events and Figure 3D shows the cumulative probability distribution of these sparks. The median and interquartile range of the distribution was  $7.6 \pm 5.7$  a.u. for single-cluster sparks and  $15.7 \pm 20.1$  a.u. for double-cluster sparks ( $P < .01$ ). Interestingly, analysis of the mass of the calcium signal for individual RyR2 clusters showed no difference between the signal mass of a single-cluster event ( $29.77 \pm 5.47$  a.u.) and the mass of the

calcium signal in RyR2 clusters that triggered the activation of a second RyR2 cluster ( $31.72 \pm 5.46$  a.u.), suggesting that the occurrence of two-cluster sparks at baseline is not determined by the calcium discharged by the initiating cluster, but more likely depends on the proximity of the second cluster to its threshold for releasing calcium spontaneously.

## 2.2 | $\beta_2$ -adrenergic stimulation induce multi-cluster activation and larger calcium spark mass

Because beta-adrenergic stimulation is known to induce arrhythmia and arrhythmic responses in cardiomyocytes, we investigated how the  $\beta_2$ -adrenergic agonist fenoterol (FENO) affected RyR2 phosphorylation and calcium signals in individual RyR2 clusters. As shown in Figure 4A, FENO doubled RyR2 phosphorylation at s2809 in mouse ventricular myocytes with GFP-tagged RyR2 (Figure 4B). FENO also increased RyR2 phosphorylation at s2815 significantly (Figure 4C). As shown in Figure 4D, the fraction of de-phosphorylated RyR2s at s2809 was also halved when myocytes were exposed to FENO. Moreover, the selective protein kinase A (PKA)-inhibitor KT5720 reverted the effect of FENO on s2809 de-phosphorylation (Figure 4D,E), suggesting that  $\beta_2$ -adrenergic stimulation increases PKA-dependent phosphorylation of the RyR2 at s2809. Analysis of calcium signals in individual RyR2 clusters and calcium spark dynamics after exposure to FENO (Figure 5A-D) revealed a four-fold increase in the frequency of sparks triggered by the activation of two RyR2 clusters and a doubling of three-cluster sparks (Figure 5E). Furthermore, FENO significantly increased the duration of both 1- and 2-cluster sparks in the presence of FENO (Figure 6A,B). This, in turn, increased the calcium spark mass of one and two-cluster sparks (Figure 6C), shifting both the probability distribution and the cumulative probability distribution towards higher spark masses (Figure 6D). Thus, the median and interquartile range of single-cluster distribution was  $13.6 \pm 16.6$  a.u. in comparison with two-cluster sparks  $20.8 \pm 17.8$  a.u. For three-cluster sparks median and interquartile range was  $26.8 \pm 16.8$  a.u. In support of

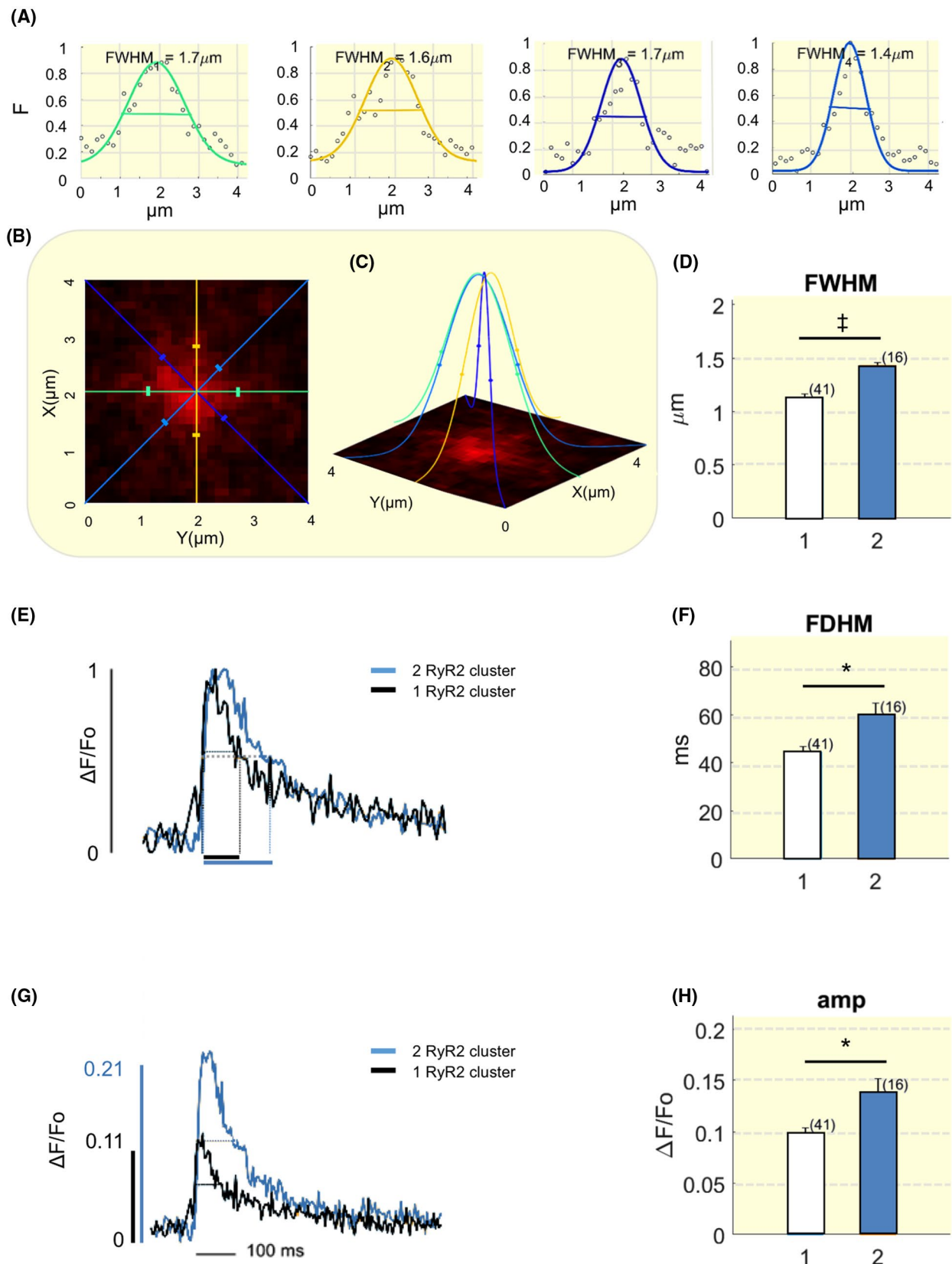


**FIGURE 2** Properties of calcium sparks resulting from the activation of one or two RyR2 clusters. A, Full width of a calcium spark at half maximum (FWHM) was measured from four profiles measured at 45° angles. B, 2D projection of a calcium spark with indication of the lines where calcium spark profiles in A were measured. C, 3D projection of the spark in B. D, FWHM for 1- and 2-cluster sparks. E, Normalized calcium transients for 1- and 2-cluster sparks with indication of the full duration at half maximum (FDHM). F, Average FDHM for 1- and 2-cluster sparks. G, Representative calcium transients for 1- and 2-cluster sparks. H, Average amplitude of 1- and 2-cluster sparks. \* $P < .05$ ;  $\dagger P < .001$  (rank-sum test). Number of cells from 16 mice is indicated in parenthesis

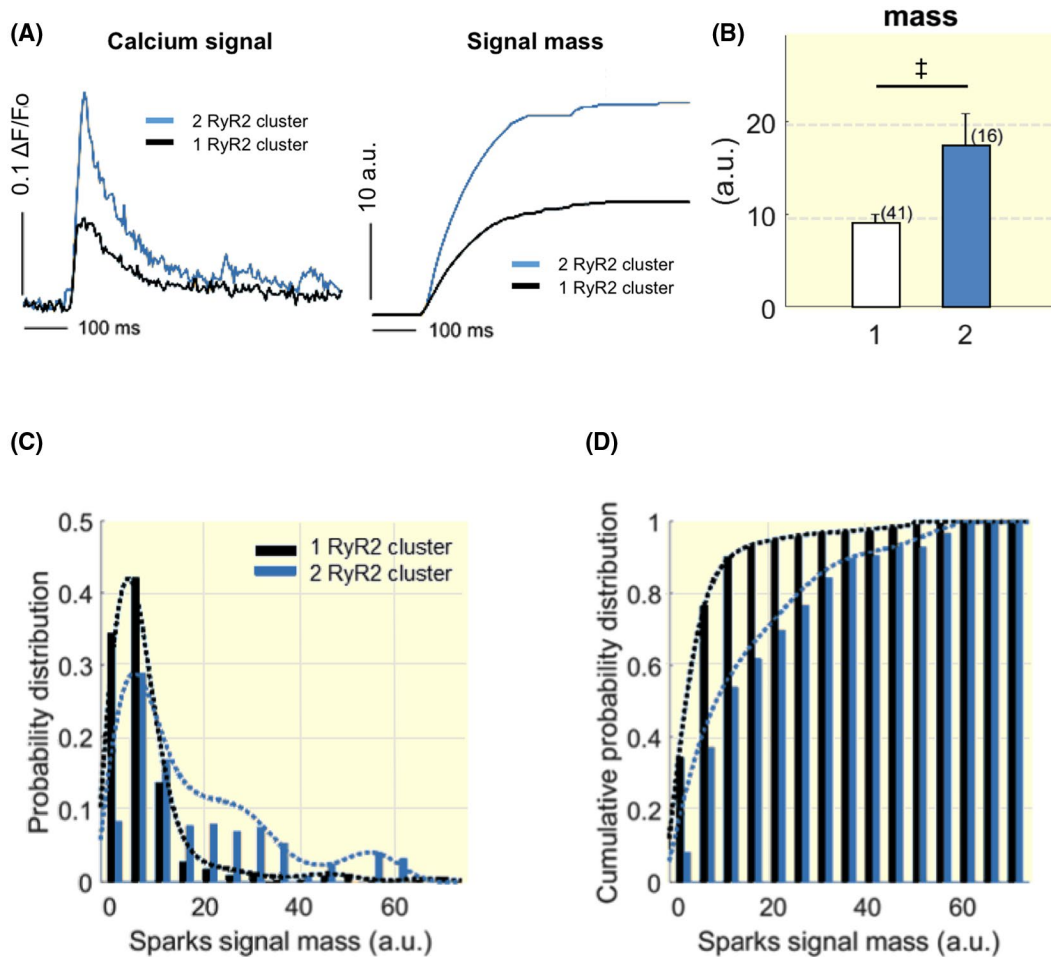


**FIGURE 3** Calcium spark signal mass and the probability distribution for one- and two-cluster sparks. A, Calcium spark traces (left) and their time integral (right) corresponding to the calcium signal mass. Signals are shown for 1- and 2-cluster sparks. B, Average spark signal mass for 1- and 2-cluster sparks. C, Probability distribution of the spark signal masses for 1- and 2-cluster sparks. D, Cumulative probability distribution of the signal masses in C. measurements were from 41 myocytes with one-cluster sparks and 16 myocytes with two-cluster sparks from 16 mice.  $\ddagger P < .001$  (rank-sum test). Dotted lines represent smoothing of the data with a kernel density estimate

the notion that these effects of FENO on signal mass facilitated the fusion of calcium signals from neighbouring RyR2 clusters, the fraction of clusters that were activated during a spontaneous calcium release event (maximal path length) increased from  $2.9\% \pm 1.1\%$  in control to  $25.5\% \pm 4.9\%$  with FENO.

Comparison of calcium signals in individual RyR2 clusters during the activation of a single or two-cluster spark showed that after exposure to FENO the amplitude ( $P < .05$ ) and mass ( $P < .01$ ) of the calcium signal was significantly larger in RyR2 clusters that triggered the activation of a second RyR2 cluster than in RyR2 clusters from single-cluster sparks. Moreover, the calcium spark frequency was higher in individual RyR2 clusters contributing to two-cluster events than in RyR2 clusters that only contributed to single-cluster events (Figure S2).

To test the influence of the SR calcium load on the incidence and properties of individual RyR2 cluster activations, we measured the caffeine-induced calcium transient

in individual RyR2 clusters before and after exposure to FENO. As shown in Figure 7A and Figure S3, FENO increased both the caffeine-induced calcium transient and the number of times a cluster is activated, suggesting that the firing frequency of an RyR2 cluster might be determined by the SR calcium load. However, analysis of calcium signals in individual RyR2 clusters revealed that clusters with spontaneous activity had lower SR calcium load than the clusters without spontaneous activity, and the relationship between SR calcium load and RyR2 cluster activity revealed that the activity was not correlated with the load. As shown in Figure 7B, this was true both for CON and FENO. By contrast, there was a weak positive correlation ( $r = 0.28$ ,  $n = 538$ ) between SR calcium load and spark mass (Figure 7C) and a strong correlation ( $R = 0.66$ ,  $n = 538$ ) between SR calcium load and amplitude (Figure 7D), suggesting that the SR calcium load determines the amount of calcium released upon activation of a RyR2 cluster. Figure 7E shows that the decay of the

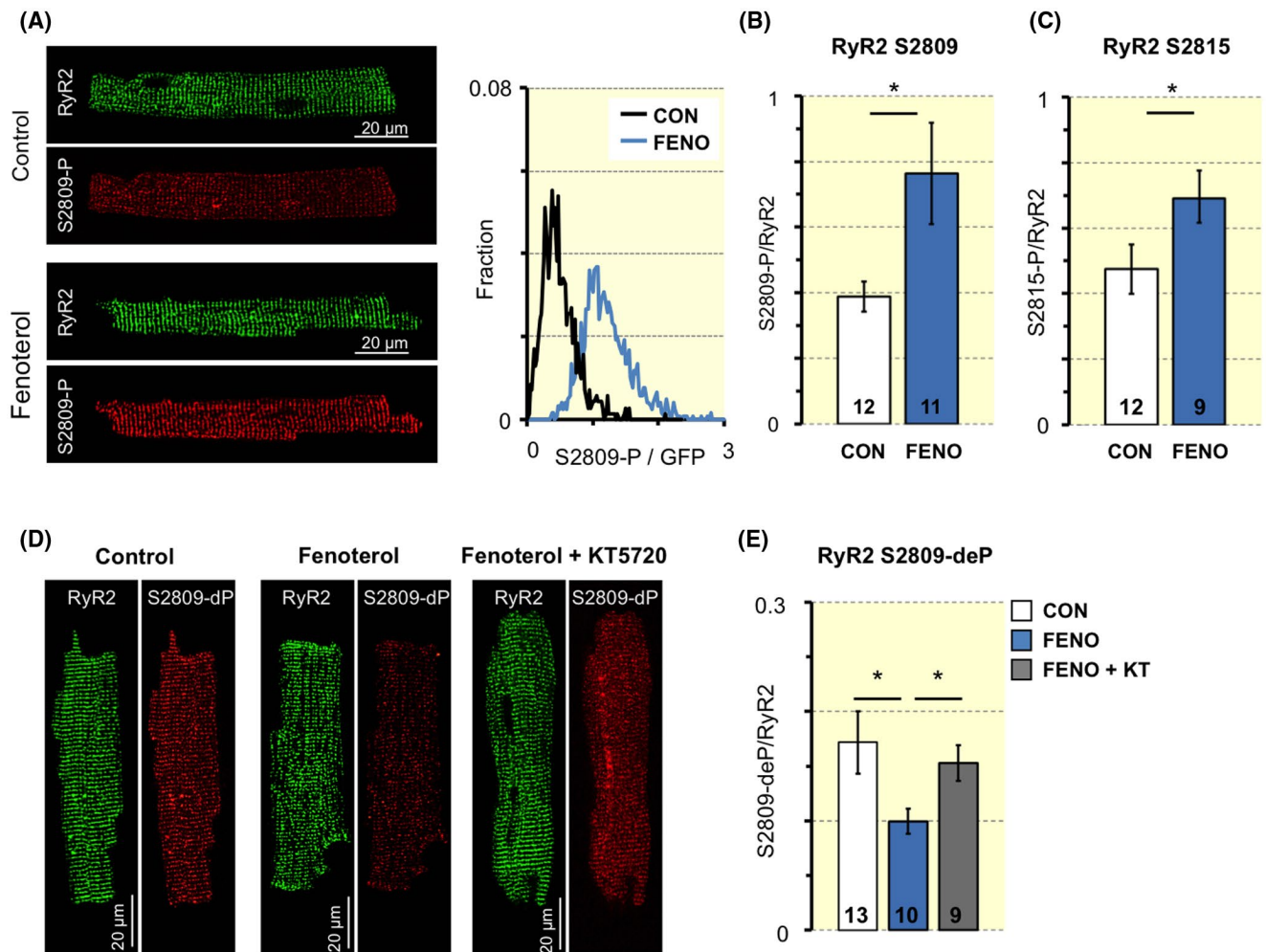


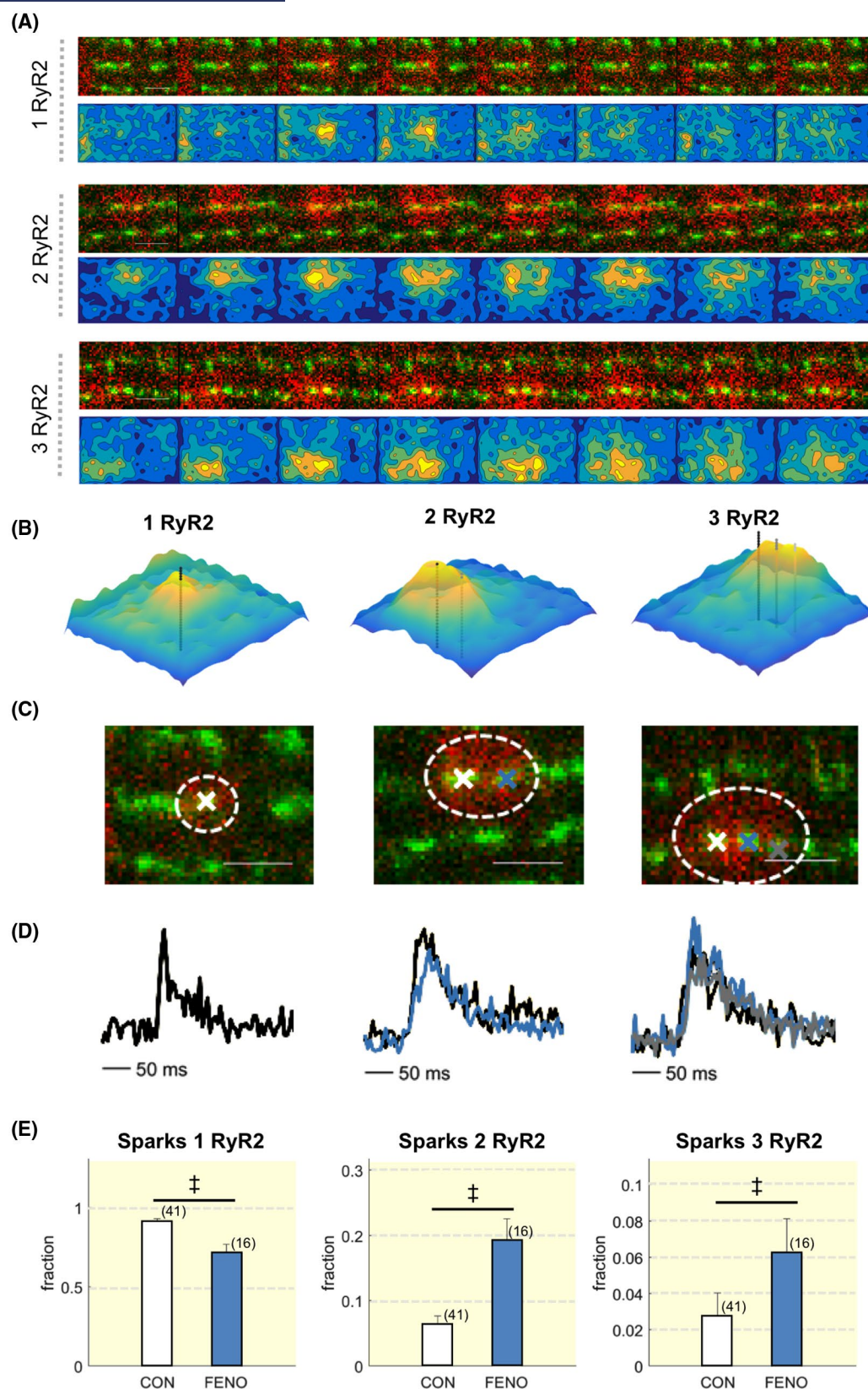
**FIGURE 4** Beta-adrenergic stimulation increases RyR2 phosphorylation at s2809 and s2815. A, Confocal images of myocytes with GFP-tagged RyR2 (green channel) and immuno-labelling of s2809 phosphorylated RyR2 (s2809-P; red channel). Images were recorded in myocytes incubated with control (CON) or 3  $\mu$ M fenoterol (FENO) solution for 5 minutes. The distribution of S2809-P/GFP ratios in myocytes exposed to CON and FENO is shown on the right. B, Mean s2809-P fluorescence intensity normalized to the GFP fluorescence emission for CON and FENO. Number of cells from 4 mice is given for each bar. C, Mean s2815-P fluorescence intensity normalized to the GFP fluorescence emission for CON and FENO. Number of cells from 5 mice is given for each bar. D, Confocal images of myocytes with GFP-tagged RyR2 (green channel) and immuno-labelling of s2809 dephosphorylated RyR2 (s2809-dP; red channel). Images were recorded in myocytes incubated with CON, FENO or FENO + 3  $\mu$ M KT5720 solution for 5 minutes. E, Mean s2809-dP fluorescence intensity normalized to the GFP fluorescence emission for CON, FENO and FENO+KT5720. Number of cells from 6 mice is given for each bar. \* $P < .05$  (unpaired  $t$  test)

calcium transient after activation of a RyR2 cluster was not correlated with the SR calcium load. Beta-adrenergic stimulation with the non-selective agonist isoproterenol (ISO) yielded qualitatively similar results (Figure S4). Neither FENO nor ISO changed baseline calcium significantly ( $\Delta F_0$  was  $-1.7\% \pm 8.1\%$  and  $3.2\% \pm 4.7\%$  for FENO and ISO respectively).

### 2.3 | Calcium spark mass in atrial fibrillation

Because atrial fibrillation is associated with increased spark frequency linked to changes in RyR2

phosphorylation at s2808, similar to the observed effects of FENO, we determined the spark mass and its probability distribution in human atrial myocytes from 36 patients without and 33 with atrial fibrillation (AF). To determine if there were species and tissue dependent differences in RyR2 cluster activation, we also measured the features of single- and double-cluster sparks in mouse right and left atrial myocytes. As shown in Table S1 single and double-cluster events in the atrial myocytes were comparable among those from left and right atrial chambers and similar to those observed in ventricular myocytes. In line with the previous findings,<sup>14</sup> Figure 8A,B shows that sparks were wider, lasted longer, and were more frequent in atrial myocytes from patients with AF (see Figure S5



for details). Consequently, AF was associated with an increase in the spark mass from  $16.9 \pm 1.9$  a.u. in patients without AF to  $25.4 \pm 2.6$  a.u. ( $P < .05$ ) in patients with AF (Figure 8C). The probability distribution of spark masses shown in Figure 8D,E revealed that sparks with

masses larger than 20 a.u. were much more frequent in AF, being the median and interquartile range of the cumulative spark mass distribution  $10.7 \pm 10.9$  a.u. for noAF and  $22.9 \pm 23.4$  a.u. for AF ( $P < .05$ ). Comparison of the cumulative probability distributions for human atrial

**FIGURE 5**  $\beta$ -adrenergic stimulation favours induction of sparks with co-activation of multiple RyR2 clusters. A, Superimposed image frames of GFP-tagged RyR2 clusters (green) and calcium spark signal (red). The colour-code map below images show the isolated calcium spark signal. Consecutive image frames are shown for a single (top panels), double (middle panels) and triple RyR2 cluster spark (bottom panels) recorded in the presence of FENO. Image frames are separated by 8.32 ms, scale bar length is 2  $\mu$ m. B, 3D contour plots of the sparks shown above. C, 2D representation of the same sparks with indication of their area (dashed circles) and individual RyR2 clusters (crosses). D, Calcium signal recordings from individual RyR2 clusters in 0.5 x 0.5  $\mu$ m ROIs for the single, double and triple-cluster spark. E, Fraction of all sparks resulting from the activation of 1, 2 or 3 RyR2 clusters.  $^{\dagger}P < .001$  (rank-sum *t* test). Number of cells from 16 mice is indicated in parenthesis

myocytes with the corresponding distributions for sparks with one or two GFP-tagged RyR2 clusters revealed that the cumulative probability distribution for no AF patients and one-cluster sparks were similar (Figure 8D). On the other hand, the cumulative probability distribution for AF myocytes reached its maximum at an even slower rate than two-cluster sparks, suggesting that more clusters are recruited in sparks from patients with AF and/or that larger amounts of calcium are released from each cluster in myocytes from these patients (Figure 8E).

Finally, to determine how the distribution of calcium spark masses in myocytes without and with AF were comparable to that of myocytes from mice with GFP-tagged RyR2s at baseline or with FENO, we compared the cumulative probability distribution of calcium spark masses in the human atrial myocytes with different combinations of 1- and 2-cluster spark mass distributions. As shown in Figure 8D bottom, the cumulative probability distribution for myocytes from patients without AF was very similar to the linear combination of 1- and 2- cluster sparks observed for GFP-tagged RyR2s at baseline. On the other hand, the bottom panel of Figure 8E shows that the cumulative probability distribution for myocytes from patients with AF was most similar to that of 2-cluster sparks recorded in the presence of FENO.

### 3 | DISCUSSION

#### 3.1 | Main findings

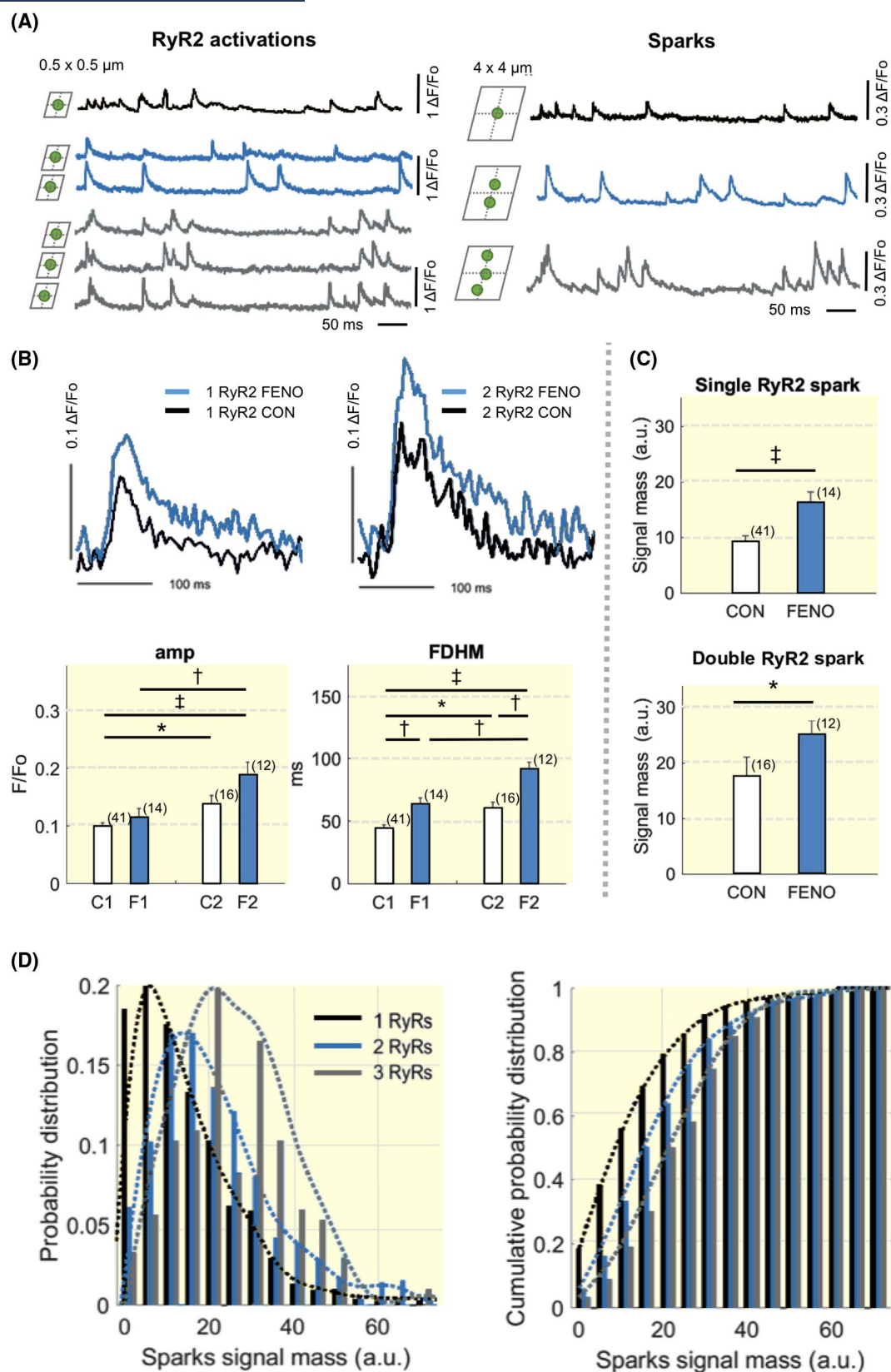
Using ventricular myocytes with GFP-tagged RyR2s, we demonstrate that the majority of calcium sparks at baseline occur when a single RyR2 cluster is activated (91.6% of all sparks). 8% of the remaining sparks occurred when two RyR2 clusters were activated. While the signal mass was doubled in these sparks, the triggering of the second RyR2 cluster was not correlated with the magnitude of the calcium signal in the first cluster, suggesting that two-cluster sparks occur randomly at baseline. By contrast,  $\beta$ -adrenergic stimulation increased the fraction of two- and three-cluster sparks and activation of a second RyR2 cluster concurred with a bigger amplitude of the calcium signal in the first cluster; demonstrating that  $\beta$ -adrenergic stimulation induces propagation of calcium release along

with neighbouring clusters, facilitating the initiation of calcium waves. Finally, the spark mass probability distribution in human atrial myocytes from patients without and with AF was similar to that observed before and after beta-adrenergic stimulation respectively, suggesting that similar mechanisms might underlie the induction of arrhythmic responses in AF.

#### 3.2 | Calcium sparks and calcium signals from individual RyR2 clusters

The frequency and kinetic properties of calcium sparks have been widely studied in both mammalian and human cardiomyocytes to address the influence of pharmacological treatments and pathological conditions on RyR2 activity and spontaneous calcium release from the SR. In particular, heart failure and cardiac arrhythmias have been associated with an increase in calcium spark frequency.<sup>1,2,7,15,16</sup> Different pharmacological treatments, such as stimulation of  $G_s$ -protein coupled receptors<sup>5,17</sup> or angiotensin receptors<sup>18</sup> have also been shown to alter the amplitude, duration or decay of sparks. Here, we show that the properties of the calcium sparks are different in sparks resulting from the activation of one and two RyR2 clusters, with the latter giving rise to macrosparks with significantly larger amplitude, width, and duration. Presumably, the combination of the cluster features determines the ability of a calcium spark to trigger larger calcium release events and arrhythmia,<sup>10,19</sup> suggesting that the mass of the calcium signal might be a good measure of the arrhythmogenic potential of a spark.

The calcium spark kinetics and signal mass, in turn, are expected to depend on both the number of RyR2s in a RyR2 cluster that is activated and the number of RyR2 clusters that fire. Indeed, several studies addressing the number of RyR2s in a RyR2 cluster, using high resolution imaging techniques in small rodents, have shown that the duration and amplitude of calcium sparks are proportional to the size of the RyR2 cluster.<sup>10</sup> On the other hand in a sheep model of AF, there was a fractioning of RyR2 clusters and a reduction in the distance to neighbouring clusters.<sup>14</sup> Here we show that, under control conditions, more than 90% of the sparks occur when a single RyR2 cluster releases calcium spontaneously while the rest of



the sparks occurred when spontaneous release from one RyR2 triggered release from its neighbour, suggesting that at baseline the calcium spark properties and signal mass is primarily determined by the number of RyR2s in the

RyR2 cluster that are activated. Moreover, the mass of the calcium signal was similar in the cluster that triggers calcium release and the cluster where calcium release was triggered, suggesting that the occurrence of two-cluster

**FIGURE 6**  $\beta$ -adrenergic stimulation increases the signal mass of calcium sparks. A, Calcium signals recorded in the presence of 3  $\mu$ M FENO from individual RyR2 clusters in  $0.5 \times 0.5 \mu\text{m}^2$  ROIs (left) and the resulting calcium spark signal in a  $4 \times 4 \mu\text{m}^2$  ROI (right). Signals are shown for a single (black trace), a double (blue traces) or a triple RyR2 cluster spark (grey traces). B, Superimposed traces of sparks with 1 or 2 RyR2 clusters in 41 control cells from 16 mice (black) and 14 cells from 7 mice with FENO (blue). Shown below are the amplitude (amp) and duration of the calcium spark signal at half maximum (FDHM) for sparks with 1 or 2 RyR2 clusters in CON (black) and with FENO (blue). C, Average time integral of the calcium spark signals in CON and with FENO. D, Probability (left) and cumulative probability distributions (right) of the signal masses for sparks with 1, 2 or 3 RyR2 clusters. Dotted lines represent smoothing of the data with a kernel density estimate. \* $P < .05$ ;  $^{\dagger}P < .01$ ;  $^{\ddagger}P < .001$  (rank-sum test)

sparks at baseline is not determined by the calcium discharged by the initiating cluster, but more likely depends on how close the second cluster is to its threshold for releasing calcium spontaneously, also referred to as the threshold for store overload induced calcium release (SOICR).<sup>20</sup>

### 3.3 | Neuro-hormonal modulation of spark mass and properties

$\beta$ -adrenergic stress has been shown to increase spontaneous calcium release in mice harbouring mutations in the RyR2<sup>15</sup> associated with increased RyR2 activity<sup>20,21</sup> and with CPVT in humans.<sup>22,23</sup> Hence,  $\beta$ -adrenergic stress might increase the calcium spark mass by increasing the RyR2 activity, the number of active RyR2s in a cluster, or the activation of multiple RyR2 clusters in each spark. In line with the former, we found that  $\beta$ 2-adrenergic stimulation increases the signal mass of sparks arising from the activation of a single RyR2 cluster. Moreover, it increased PKA-dependent phosphorylation of the RyR2 at s2809 and phosphorylation at s2815 that increases RyR2 open probability,<sup>2,4,5</sup> suggesting that the increased spark mass in single-cluster sparks may be caused by increased RyR2 activity in the cluster. On the other hand,  $\beta$ 2-adrenergic stimulation also increased SR calcium load, and there was a correlation between calcium load and the amplitude of the released calcium, suggesting increased signal mass in a RyR2 cluster may be caused by both higher SR calcium load and increased RyR2 opening. Moreover, there was a three-fold increase in double- and triple-cluster sparks in myocytes subjected to  $\beta$ 2-adrenergic stimulation, suggesting that it doubles the calcium spark mass by increasing both the RyR2 activity in a cluster and by the activation of multiple RyR2 clusters. In line with previous studies, suggesting that SR calcium load regulates the calcium spark frequency,<sup>24</sup> we found that beta-adrenergic stimulation increased the global SR calcium load and RyR2 cluster firing. However, analysis of spontaneous activity and SR calcium load in individual RyR2 clusters, shown in Figure 7B, revealed that here was no correlation between SR calcium load and RyR2 cluster activity, supporting the notion that RyR2 phosphorylation determines

the activation frequency of a RyR2 cluster while the SR calcium load modulates the amplitude of the calcium released upon activation of the RyR2 cluster.

Interestingly, when subjected to  $\beta$ 2-adrenergic stimulation, the RyR2 cluster that triggered the activation of a neighbouring RyR2 cluster had a significantly larger mass than the cluster that was triggered. This pattern indicates a shift from random activation of neighbouring clusters at baseline to triggered activation of RyR2 clusters under  $\beta$ 2-adrenergic stimulation that may facilitate the formation and propagation of calcium waves. In line with this notion, FENO and ISO increased the maximal path length for a spontaneous calcium release event 8.7- and 9.9-fold respectively.

### 3.4 | Relationship between calcium spark mass and atrial fibrillation

Because cardiac arrhythmia and heart failure have been associated with an increase in RyR2 phosphorylation and spontaneous calcium release events,<sup>1,4,7,15,25,26</sup> the presence of these features is often considered to indicate risk of arrhythmia. However, overexpression of constitutively active calmodulin kinase, expected to increase RyR2 phosphorylation at s2815 in mice, was found to suppress calcium spark and waves.<sup>27</sup> Similarly, overexpression of phospholamban in mice harbouring the RyR2 mutation R4496C dramatically increased spontaneous calcium release events but prevented arrhythmogenesis because large calcium waves observed in R4496C mice were split into smaller but more frequent release events, ie with a smaller mass, unable to induce spontaneous electrical activity in the double mutant mice.<sup>8</sup> Similar to this, the present analysis of spontaneous calcium release events at the level of individual RyR2 clusters shows that the cumulative probability distribution of the calcium spark masses in a myocyte population may be more robust than the spark frequency to assess the risk of arrhythmia. In support of these hypotheses the cumulative probability distribution of the spark mass was shifted towards higher spark masses in atrial myocytes from patients with AF and upon  $\beta$ -adrenergic stimulation, which also induces calcium waves and transient arrhythmia at the cellular level<sup>28</sup> and is used to identify ectopic foci in patients undergoing ablation of AF.<sup>29</sup> Further support for an association between calcium spark

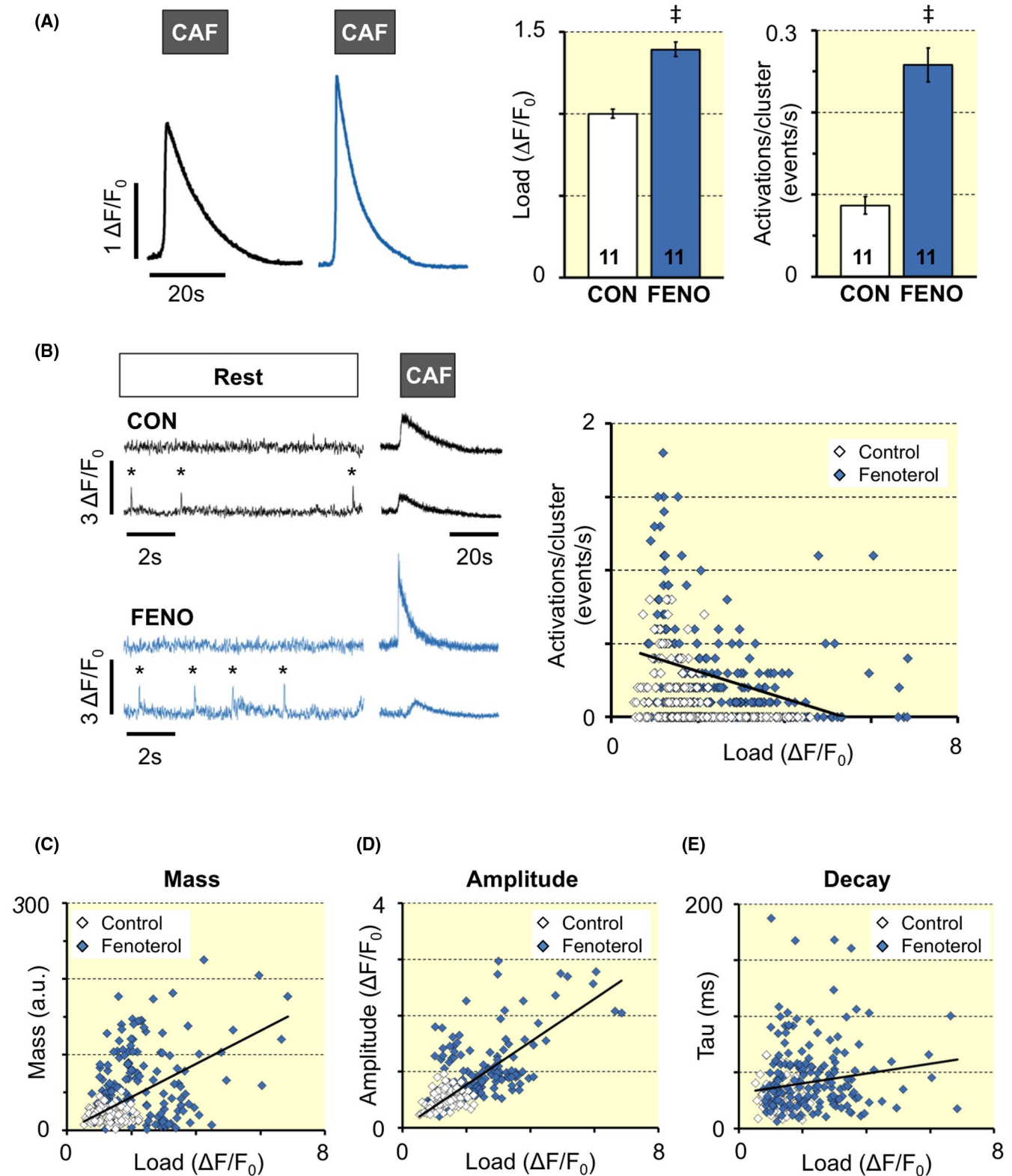


**FIGURE 7** Increased SR calcium load does not increase RyR2 cluster activation. A, Representative caffeine (CAF) induced calcium transients recorded before (CON) and after exposure to fenoterol (FENO). Mean SR calcium load, measured as the amplitude of the transients and mean number of activations per cluster is shown on the right. Number of cells from four mice are given for each bar. B, Calcium signals in single RyR2 clusters in CON and FENO at rest and upon exposure to caffeine. Notice that the amplitude of the caffeine-induced calcium transient was smaller in the clusters with spontaneous activity than in those without activity. The relationship between amplitude (SR calcium load) and cluster activity is shown on the right for 269 RyR2 clusters. C-E, Relationship between SR calcium load and the mass (C), amplitude (D) and decay (E) of calcium signals from single RyR2 cluster activations.  $^{\ddagger}P < .001$  using paired  $t$  test for load and rank-sum test for activations/cluster

mass and arrhythmogenic calcium release is afforded by the finding that flecainide, which prevents catecholaminergic polymorphic ventricular tachycardia in a transgenic mouse model and in humans,<sup>30</sup> increases the frequency of calcium sparks but reduces their mass in the mouse model.<sup>31</sup> By

contrast, tetracaine, which reduces the frequency but not the mass of calcium sparks, is unable to prevent arrhythmogenic calcium release events in the same mouse model.<sup>30,31</sup>

Analysis of the calcium spark mass in human atrial myocytes revealed that myocytes from patients without a

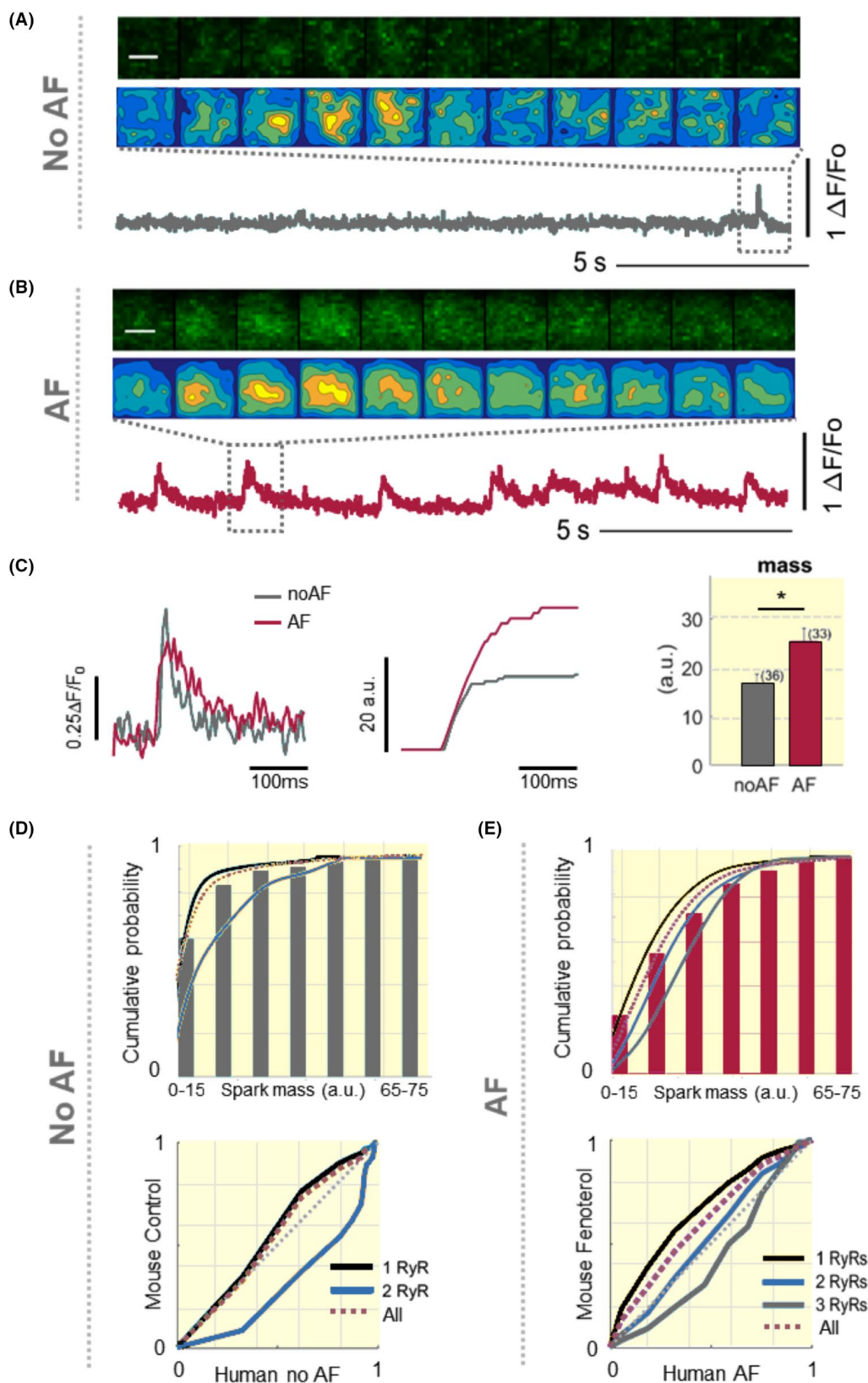


**FIGURE 8** Calcium spark mass is bigger and more diverse in patients with than without AF. A, Consecutive image frames recorded during a calcium spark in myocytes from a patient without AF (No AF). Colour-coded calcium sparks are shown in the middle and calcium trace with indication (dashed rectangle) of the spark where images were collected is shown below. Image frames are separated by 11.63 ms, scale bar is 2  $\mu\text{m}$ . B, Same representation as in A from a patient with AF. C, Superimposed spark signals (left) and their time integral (middle) from a patient without and with AF. The average time integral of sparks (mass) is shown on the right for 36 No AF and 33 AF patients that had sparks.  $*P < .05$  (rank-sum test) D-E, Cumulative probability distribution of spark masses in patients without (D) and with AF (E). The mass distribution for sparks from mice with 1 (black trace), 2 GFP-tagged RyR2 clusters (blue trace) or all sparks (brown dotted trace) are superimposed on the no AF distribution. The mass distribution for sparks in mice treated with 3  $\mu\text{M}$  FENO that had 1 (black trace), 2 (blue trace), 3 GFP-tagged RyR2 clusters (grey trace), or all sparks (purple dotted trace) are superimposed on the AF distribution. Corresponding Q-Q plots are shown at the bottom for control mice vs patients without AF (D) and for FENO treated mice vs patients with AF (E)

history of atrial fibrillation had a calcium spark mass and a cumulative probability distribution of the spark mass that was similar to the linear combination of one and two-cluster sparks recorded at baseline in mouse myocytes with GFP-tagged RyR2s. By contrast, the calcium spark mass was twice as big in patients with atrial fibrillation and the cumulative probability distribution of the spark mass was shifted from a median of 12a.u. in patients without AF to 23 a.u. in those with the arrhythmia, which is even larger than the linear combination of single, double and three-cluster sparks recorded in mouse myocytes with GFP-tagged RyR2s under  $\beta$ -adrenergic stimulation. These findings document that  $\beta$ -adrenergic stimulation mimics the higher incidence and mass of calcium sparks in myocytes from patients with AF. However, our findings also suggest that additional pathological alterations in the calcium homeostasis are required to achieve the accumulated probability distribution and median spark mass observed in AF.

### 3.5 | Study limitations

Because of ethical considerations and limitations in the availability of human atrial tissue samples, isolation of human atrial myocytes is only feasible in right atrial tissue samples from patients undergoing surgical interventions that require extracorporeal circulation; and some of the observations from right atrial myocytes might differ from those of left atrial myocytes. Moreover, we cannot exclude that concurrent cardiovascular disease and pharmacological treatments of the tissue donors might influence our findings in human atrial myocytes. Furthermore, the measurements of calcium signals with confocal imaging are limited by the position of the spark relative to the confocal plane and presumably out of focus sparks introduce some noise in the measurements of cluster activations and spark features. Similarly, our confocal microscope does not allow distinguishing between multiple small RyR2 clusters and a supercluster and we cannot exclude that some clusters with large signal masses could contain several small RyR2 clusters with inter-cluster distances below the spatial resolution. Finally, a reliable characterization

of the cumulative probability distribution of the spark masses requires a considerable number of sparks from a reasonable number of patients in order to avoid that a large number of sparks in a few cells or patients biases the spark mass distribution. To minimize this issue, we used a larger number of myocytes from patients without a history of AF where calcium sparks were less abundant.

## 4 | CONCLUSIONS

In conclusion, our findings show that calcium sparks at baseline are largely caused by the activation of a single RyR2 cluster in GFP-tagged mouse ventricular myocytes. Moreover, our results suggest that the calcium spark mass and the cumulative probability distribution of the spark mass may be better measures of the arrhythmogenic potential of calcium sparks than their frequency. In agreement with this notion, calcium spark masses and their cumulative probability distribution in atrial myocytes from patients without AF was similar to that observed at baseline in myocytes with GFP-tagged RyR2s, while  $\beta$ -adrenergic stimulation, which is commonly used to induce arrhythmogenic calcium release, favoured co-activation of multiple RyR2 clusters in a spark, increased the maximal path length of propagating calcium release events and increased the spark mass as well as its probability distribution towards values observed in atrial myocytes from patients with AF. These findings also suggest that antiarrhythmic strategies for the treatment of AF may benefit from identifying compounds that shift the cumulative probability distribution towards lower calcium spark masses.

## 5 | MATERIALS AND METHODS

### 5.1 | Myocyte preparation

Mouse ventricular myocytes (MVM) were isolated from transgenic mice overexpressing GFP-tagged RyR2<sup>32</sup> using Langendorff perfusion of the whole heart with an enzymatic solution as previously described.<sup>32</sup> Mice were

sacrificed using cervical dislocation after general anaesthesia with intraperitoneal administration of ketamine (75 mg/kg) and Medetomidine (1 mg/kg). The study was approved by the Bioethical Committee at Hospital de Sant Pau (AF-RISK\_2015) and authorized by Generalitat de Catalunya. The study conforms to the Guide for the Care and Use of Laboratory Animals published by the US National Institutes of Health. Only elongated cardiomyocytes with clear cross striations and without abnormal granulation were used.

Human atrial myocytes (HAM). Right atrial myocardial samples were collected from 86 patients undergoing cardiac surgery with extracorporeal circulation. Each patient gave written consent to obtain a tissue sample that would otherwise have been discarded during the surgical intervention. The study was approved by the ethical committee of Hospital de la Santa Creu i Sant Pau, Barcelona (AF-RISK\_2015) and the investigation conforms to the principles outlined in the Declaration of Helsinki. After excision of the atrial sample, it was cut into small fragments and atrial myocytes were isolated as previously described.<sup>33</sup>

## 5.2 | Confocal calcium imaging

Human atrial myocytes and mouse ventricular myocytes were imaged using a resonance-scanning confocal microscope (Leica SP5 AOBS) with a 63x glycerol-immersion objective. Fluorophores were excited with a HeNe laser (100 mW) or an Argon laser (1 mW), and the laser power was set to 20% of the maximum.

HAMs were loaded with 2.5  $\mu\text{M}$  fluo-4 AM. The fluorophore was excited at 488 nm and emission was collected between 500 and 650 nm using a Leica Hybrid Detector. Laser attenuation was set to 4%. Image sequences of 2497 frames with a 1.7x digital zoom factor were obtained at dimensions of 512 x 140 pixels with a pixel size of 0.28 x 0.28  $\mu\text{m}$  and frame time of 11.63 ms yielding a total duration of 29.04 s. The experiments were performed at room temperature.

In order to establish the relationship between the activation of individual RyR2 clusters and calcium spark frequency or properties, we used the fluorescent calcium indicator Rhod-2 to monitor the activation of individual RyR2 clusters in isolated MVM from mice with GFP-tagged RyR2 clusters. Cells were loaded with 5  $\mu\text{M}$  Rhod-2 AM for 40 minutes. The digital zoom factor was increased to 8X and the image dimension was reduced to 40 x 256 pixels in order to obtain a good compromise between temporal resolution and pixel size, ie 4.16 ms and 0.1 x 0.1  $\mu\text{m}$  respectively. GFP was excited with a 488 nm Argon laser attenuated at 5% and emission was collected between 495 and 535 nm with a Leica photomultiplier tube (PMT). Rhod-2 was excited with a HeNe laser at 543 nm attenuated at 8% and its emission was collected between 600 and 750 nm with the

Leica Hybrid detector. MVM experiments were performed at 37°C. Beta-adrenergic stimulation was induced by exposing myocytes to the  $\beta$ 2-adrenergic agonist fenoterol (3  $\mu\text{M}$ ) or the non-selective agonist isoproterenol (ISO).

## 5.3 | Immunofluorescent labelling

Isolated GFP-tagged mouse ventricular myocytes were fixed with paraformaldehyde for 10 minutes at room temperature. Subsequently, cells were labelled with the primary antibodies rabbit anti-ser2809-P, rabbit anti-ser2809-deP or anti-ser2815-P as previously described.<sup>34</sup> After labelling, cells were washed again and stored at 4°C until imaging (see supplementary methods for further details). GFP-tagged RyR2 clusters were visualized using excitation at 488nm (attenuated to 5%) and collection of fluorescence emission between 495 and 538 nm. S2809 phosphorylated clusters were visualized using excitation at 543 nm (attenuated to 10%) and collection of fluorescence emission between 580 and 750 nm. Total and phosphorylated RyR2 clusters were detected using a custom-made algorithm as previously described<sup>35</sup> and the degree of RyR2 phosphorylation at s2809 was calculated as the fluorescence intensity ratios s2809/GFP for each RyR2 cluster (see supplementary methods).

## 5.4 | Image processing

Images were exported from Leica Image File format using the Bio-Formats libraries.<sup>36</sup> A custom-made image processing pipeline was designed to automatically detect calcium release events at different spatial and temporal scales and to characterize them using a series of morphological and kinetic attributes. The detection algorithms were developed using MATLAB (The MathWorks, Boston).

Different event detection and characterization algorithms were developed to analyse MVM and HAM experiments. Next, is a simplified itemization of the main processing pipeline (see supplementary methods for further details).

1. Spatial localization of RyR2 clusters (amplitude thresholding and detection of local maxima).
2. Extraction of the average fluorescence signal in a 0.5  $\mu\text{m}$  x 0.5  $\mu\text{m}$  region of each RyR2 cluster.
3. Detection of RyR2 cluster activations using a continuous wavelet transform with temporal support of 500 ms
4. Characterization of individual RyR2 cluster activations (amplitude, kinetics and mass of events).
5. Hierarchical clustering in order to group simultaneous activations of multiple RyR2 cluster, within a spatial

and temporal window of 2  $\mu\text{m}$  and 50 ms, into spark events.

6. Measure the average fluorescence signal of spark events in a 4 $\mu\text{m}$  x 4 $\mu\text{m}$  region centred at the centroid of the activated RyR2 clusters.
7. Characterization of individual sparks (size, amplitude, kinetics and mass).

The signal mass of both RyR2 activation and spark events was obtained by calculating the integral of normalized fluorescence signal above the baseline level,

$$\text{signal mass} = \int_{t_1}^{t_i} F(t) - bl(t) dt.$$

The baseline signal  $bl(t)$  was determined using a linear interpolation between the initial and final baseline levels of the event, and the temporal window to integrate the mass starts at the calcium up rise ( $t_1$ ) and lasts four times the FDHM of the spark ( $t_i$ ). The spatial extent of the mass is taken into account in the region of interest (ROI) used to obtain the average event signal  $F(t)$ , ie, a 0.5  $\mu\text{m}$  x 0.5  $\mu\text{m}$  ROI for the RyR2 cluster activation events and a 4  $\mu\text{m}$  x 4  $\mu\text{m}$  ROI for the spark events.

Image artefacts, spontaneous transients and calcium waves were discarded from the detected RyR2 cluster event candidates by requiring a set of predefined morphological properties (see supplementary methods). In particular, the signal amplitude was a critical parameter for separating RyR2 cluster activations from noise and candidate events were required to have an amplitude that was at least twice the standard deviation of the baseline noise. Moreover, events that had a full duration at half maximum larger than 250 ms or decay times longer than 200 ms were discarded.

## 5.5 | Statistical analysis

Data were analysed in accordance with Acta Physiologica guidelines for good publishing practice<sup>37</sup> and data from the RyR2s activations and sparks analysis was analysed in MATLAB. In the paper, the reported values of the parameters are the average of each cell  $\pm$  standard error. Distributions are characterized by the median and interquartile range. For cluster activation and calcium sparks, all comparisons between groups were performed using a non-parametric Wilcoxon rank-sum test since the observations were not normally distributed (Kolmogorov-Smirnov normality test). Statistical tests and significance levels are given in each figure and expressed as  $P$ -values or \*, meaning  $P < .05$ , † for  $P < .01$  and ‡ for  $P < .001$ .

## ACKNOWLEDGEMENTS

The collaboration of the Cardiac Surgery Team at Hospital de la Santa Creu i Sant Pau and the assistance of Mr Søren M. Almendros with calcium image analysis is greatly appreciated.

## CONFLICTS OF INTEREST

Authors have no conflicts of interest to declare.

## DATA AVAILABILITY STATEMENT

The human data that support the findings of this study are not publicly available Because of privacy or ethical restrictions. Other data are available from the corresponding author upon reasonable request.

## ORCID

Leif Hove-Madsen  <https://orcid.org/0000-0001-5493-3998>

## REFERENCES

1. Hove-Madsen L, Llach A, Bayes-Genis A, et al. Atrial fibrillation is associated with increased spontaneous calcium release from the sarcoplasmic reticulum in human atrial myocytes. *Circulation*. 2004;110(11):1358-1363.
2. Voigt N, Li N, Wang Q, et al. Enhanced sarcoplasmic reticulum  $\text{Ca}^{2+}$  leak and increased  $\text{Na}^{+}$ - $\text{Ca}^{2+}$  exchanger function underlie delayed afterdepolarizations in patients with chronic atrial fibrillation. *Circulation*. 2012;125(17):2059-2070.
3. Burashnikov A, Antzelevitch C. Reinduction of atrial fibrillation immediately after termination of the arrhythmia is mediated by late phase 3 early afterdepolarization-induced triggered activity. *Circulation*. 2003;107(18):2355-2360.
4. Vest JA, Wehrens XH, Reiken SR, et al. Defective cardiac ryanodine receptor regulation during atrial fibrillation. *Circulation*. 2005;111(16):2025-2032.
5. Llach A, Molina CE, Prat-Vidal C, et al. Abnormal calcium handling in atrial fibrillation is linked to up-regulation of adenosine  $\text{A}_2\text{A}$  receptors. *Eur Heart J*. 2011;32(6):721-729.
6. Neef S, Dybkova N, Sossalla S, et al.  $\text{CaMKII}$ -dependent diastolic SR  $\text{Ca}^{2+}$  leak and elevated diastolic  $\text{Ca}^{2+}$  levels in right atrial myocardium of patients with atrial fibrillation. *Circ Res*. 2010;106(6):1134-1144.
7. Ai X, Curran JW, Shannon TR, Bers DM, Pogwizd SM.  $\text{Ca}^{2+}$ /calmodulin-dependent protein kinase modulates cardiac ryanodine receptor phosphorylation and sarcoplasmic reticulum  $\text{Ca}^{2+}$  leak in heart failure. *Circ Res*. 2005;97(12):1314-1322.
8. Bai Y, Jones PP, Guo J, et al. Phospholamban knockout breaks arrhythmogenic  $\text{Ca}^{2+}$  waves and suppresses catecholaminergic polymorphic ventricular tachycardia in mice. *Circ Res*. 2013;113(5):517-526. doi:10.1161/CIRCRESAHA.113.301678
9. Soeller C, Crossman D, Gilbert R, Cannell M b. Analysis of ryanodine receptor clusters in rat and human cardiac myocytes. *Proc Natl Acad Sci USA*. 2007;104(38):14958-14963. doi:10.1073/pnas.0703016104
10. Galice S, Xie Y, Yang Y, Sato D, Bers DM. Size matters: ryanodine receptor cluster size affects arrhythmogenic sarcoplasmic reticulum calcium release. *J Am Heart Assoc*. 2018;7(13):8724.

11. Lipp P, Niggli E. Submicroscopic calcium signals as fundamental events of excitation-contraction coupling in guinea-pig cardiac myocytes. *J Physiol.* 1996;492(1):31-38. doi:10.1113/jphysiol.1996.sp021286
12. Cheng H, Lederer WJ, Cannell MB. Calcium sparks: elementary events underlying excitation-contraction coupling in heart muscle. *Science.* 1993;262(5134):740-744.
13. Bolton TB, Imaizumi Y. Spontaneous transient outward currents in smooth muscle cells. *Cell Calcium.* 1996;20(2):141-152. doi:10.1016/S0143-4160(96)90103-7
14. Macquaide N, Tuan HTM, Hotta JI, et al. Ryanodine receptor cluster fragmentation and redistribution in persistent atrial fibrillation enhance calcium release. *Cardiovasc Res.* 2015;108(3):387-398. doi:10.1093/cvr/cvv231
15. Lehnart SE, Wehrens XH, Laitinen PJ, et al. Sudden death in familial polymorphic ventricular tachycardia associated with calcium release channel (ryanodine receptor) leak. *Circulation.* 2004;109(25):3208-3214.
16. Voigt N, Heijman J, Wang Q, et al. Cellular and molecular mechanisms of atrial arrhythmogenesis in patients with paroxysmal atrial fibrillation. *Circulation.* 2014;129(2):145-156.
17. Ghigo A, Perino A, Mehel H, et al. Phosphoinositide 3-kinase  $\gamma$  protects against catecholamine-induced ventricular arrhythmia through protein kinase A-mediated regulation of distinct phosphodiesterases. *Circulation.* 2012;126(17):2073-2083. doi:10.1161/CIRCULATIONAHA.112.114074
18. Gassanov N, Brandt MC, Michels G, Lindner M, Er F, Hoppe UC. Angiotensin II-induced changes of calcium sparks and ionic currents in human atrial myocytes: potential role for early remodeling in atrial fibrillation. *Cell Calcium.* 2006;39(2):175-186.
19. Kolstad TR, van den Brink J, MacQuaide N, et al. Ryanodine receptor dispersion disrupts  $\text{Ca}^{2+}$  release in failing cardiac myocytes. *eLife.* 2018;7:39427. doi:10.7554/eLife.39427
20. Jiang D, Xiao B, Yang D, et al. RyR2 mutations linked to ventricular tachycardia and sudden death reduce the threshold for store-overload-induced  $\text{Ca}^{2+}$  release (SOICR). *Proc Natl Acad Sci USA.* 2004;101(35):13062-13067.
21. Jiang D, Xiao B, Zhang L, Chen SR. Enhanced basal activity of a cardiac  $\text{Ca}^{2+}$  release channel (ryanodine receptor) mutant associated with ventricular tachycardia and sudden death. *Circ Res.* 2002;91(3):218-225.
22. Priori SG, Napolitano C, Tiso N, et al. Mutations in the cardiac ryanodine receptor gene (hRyR2) underlie catecholaminergic polymorphic ventricular tachycardia. *Circulation.* 2001;103(2):196-200. doi:10.1161/01.CIR.103.2.196
23. Laitinen PJ, Brown KM, Piippo K, et al. Mutations of the cardiac ryanodine receptor (RyR2) gene in familial polymorphic ventricular tachycardia. *Circulation.* 2001;103(4):485-490.
24. Cheng H, Lederer MR, Lederer WJ, Cannell MB. Calcium sparks and  $[\text{Ca}^{2+}]_i$  waves in cardiac myocytes. *Am J Physiol Cell Physiol.* 1996;270(1):C148-C159. doi:10.1152/ajpcell.1996.270.1.C148
25. Sossalla S, Fluschnik N, Schotola H, et al. Inhibition of elevated  $\text{Ca}^{2+}$ /calmodulin-dependent protein kinase II improves contractility in human failing myocardium. *Circ Res.* 2010;107(9):1150-1161.
26. Reiken S, Wehrens XH, Vest JA, et al. Beta-blockers restore calcium release channel function and improve cardiac muscle performance in human heart failure. *Circulation.* 2003;107(19):2459-2466.
27. Yang D, Zhu WZ, Xiao B, et al.  $\text{Ca}^{2+}$ /calmodulin kinase II-dependent phosphorylation of ryanodine receptors suppresses  $\text{Ca}^{2+}$  sparks and  $\text{Ca}^{2+}$  waves in cardiac myocytes. *Circ Res.* 2007;100(3):399-407. doi:10.1161/01.RES.0000258022.13090.55
28. Fujiwara K, Tanaka H, Mani H, Nakagami T, Takamatsu T. Burst emergence of intracellular  $\text{Ca}^{2+}$  waves evokes arrhythmogenic oscillatory depolarization via the  $\text{Na}^{+}$ - $\text{Ca}^{2+}$  exchanger: simultaneous confocal recording of membrane potential and intracellular  $\text{Ca}^{2+}$  in the heart. *Circ Res.* 2008;103(5):509-518.
29. Isa-Param R, Pérez-Castellano N, Villacastin J, et al. Inducibility of atrial arrhythmias after adenosine and isoproterenol infusion in patients referred for atrial fibrillation ablation. *Revista Española De Cardiología (English Edition).* 2006;59(6):559-566. doi:10.1016/S1885-5857(07)60007-3
30. Watanabe H, Chopra N, Laver D, et al. Flecainide prevents catecholaminergic polymorphic ventricular tachycardia in mice and humans. *Nat Med.* 2009;15(4):380-383. doi:10.1038/nm.1942
31. Hilliard FA, Steele DS, Laver D, et al. Flecaïnide inhibits arrhythmogenic  $\text{Ca}^{2+}$  waves by open state block of ryanodine receptor  $\text{Ca}^{2+}$  release channels and reduction of  $\text{Ca}^{2+}$  spark mass. *J Mol Cell Cardiol.* 2010;48(2):293-301. doi:10.1016/j.yjmcc.2009.10.005
32. Hiess F, Detampel P, Nolla-Colomer C, et al. Dynamic and irregular distribution of RyR2 clusters in the periphery of live ventricular myocytes. *Biophys J.* 2018;114(2):343-354. doi:10.1016/j.bpj.2017.11.026
33. Hove-Madsen L, Prat-Vidal C, Llach A, et al. Adenosine A2A receptors are expressed in human atrial myocytes and modulate spontaneous sarcoplasmic reticulum calcium release. *Cardiovasc Res.* 2006;72(2):292-302.
34. Herraiz-Martínez A, Llach A, Tarifa C, et al. The 4q25 variant rs13143308T links risk of atrial fibrillation to defective calcium homeostasis. *Cardiovasc Res.* 2019;115(3):578-589. doi:10.1093/cvr/cvy215
35. Vallmitjana A, Nolla C, Herraiz-Martínez A, Hove-Madsen L, Benítez R. Spatial localization of ryanodine receptors in human cardiac cells. In: Proceedings of the Annual International Conference of the IEEE Engineering in Medicine and Biology Society, EMBS. 2015. doi:10.1109/EMBC.2015.7319832
36. Linkert M, Rueden CT, Allan C, et al. Metadata matters: access to image data in the real world. *J Cell Biol.* 2010;189(5):777-782. doi:10.1083/jcb.201004104
37. Persson PB. Good publication practice in physiology 2019. *Acta Physiol.* 2019;227(4):13405. doi:10.1111/apha.13405

## SUPPORTING INFORMATION

Additional supporting information may be found in the online version of the article at the publisher's website.

**How to cite this article:** Nolla-Colomer C, Casabella-Ramon S, Jimenez-Sabado V, et al.  $\beta_2$ -adrenergic stimulation potentiates spontaneous calcium release by increasing signal mass and co-activation of ryanodine receptor clusters. *Acta Physiol.* 2022;234:e13736. doi:[10.1111/apha.13736](https://doi.org/10.1111/apha.13736)